



We are Nitinol.™

Effects of Hydrogen on the Phases and Transition Temperatures of NiTi

Runciman, Chen, Pelton, Trepenier

Proceedings of the International Conference on Shape Memory and Superelastic
Technologies, SMST-2006

2006

Effects of Hydrogen on the Phases and Transition Temperatures of NiTi

Amanda Runciman¹, Katherine C. Chen¹, Alan R. Pelton², Christine Trépanier²

(1) Department of Materials Engineering, California Polytechnic State University, San Luis Obispo, CA 93407, (2) Nitinol Devices & Components, 47533 Westinghouse Dr. Fremont, CA 94539

Abstract

Austenitic NiTi samples were cathodically charged with hydrogen to produce concentrations ranging from a baseline value of 9 wppm to 650 wppm. The effect of hydrogen on the phases and transition temperatures of NiTi was studied with X-ray diffraction (XRD), differential scanning calorimetry (DSC), tensile testing, and scanning electron microscopy (SEM). XRD analyses showed the B2 peaks shifting to lower 2θ angles with increased hydrogen content. The shift in 2θ angles represented an increase in the lattice parameter from 3.011 to 3.018 Å (0.7% volume increase) between 9 and 647 wppm hydrogen. DSC analyses showed a decrease in the transition temperatures and enthalpies for both the austenite and martensite phases. In the austenite phase the A_s was lowered by 8°C, the A_f by 9°C, and the enthalpy by 13 mJ/mg between 9 and 240 wppm hydrogen. The impact was more significant in the martensite phase where the M_s was lowered by 80°C, the M_f by 110°C, and the enthalpy by 11 mJ/mg between 9 and 200 wppm. Tensile testing of baseline material and hydrogen charged samples showed an increase of approximately 60 MPa in the martensite stress plateau. SEM analyses showed a transition from a ductile to brittle fracture mode with increasing hydrogen content.

Keywords

Nitinol, Hydrogen, X-ray Diffraction, Differential Scanning Calorimetry, Phase Transformation, Fracture

Introduction

Common applications of Nitinol, including many biomedical devices, rely on the unique shape memory and superelastic properties of the material. These properties depend on the austenite to martensite phase transition that occurs in NiTi. Since the transition behavior of this material is critical to its successful use, it is important to understand how the transition is affected by standard processing methods. NiTi medical devices often undergo processing steps such as cathodic cleaning with NaOH, electropolishing in acids, etching in acids, and heat treatments where it is possible for the hydrogen content of the material to be increased. Therefore, the effect of hydrogen on the phases and transitions in NiTi is a key concern in the performance of the material.

Similar to other titanium based-alloys, hydrogen embrittlement has been observed in NiTi at concentrations of approximately 100 wppm (0.01 wt.%) [1]. Hydrogen has been reported to cause a decrease in the ductility [2,3], a loss of the shape memory properties [2], and a decrease in the fatigue life [4] of NiTi. Studies have also shown that the ductility and strength in NiTi are reduced beginning at nominal concentrations (approximately 10 – 50 wppm) of hydrogen [3,5-6]. Although it is known that hydrogen affects many of the properties of NiTi, to date there have been no systematic studies of how low concentrations (< 650 wppm) of hydrogen effect the phase transitions. The purpose of this investigation is to examine how these low concentrations of hydrogen affect the stability of the austenite and martensite phases and the phase transitions through X-ray diffraction, differential scanning calorimetry, and fracture analysis.

Background

The effect of absorbed hydrogen on the B2 structure in NiTi has been studied by both Buchner *et al.* [7] and Pelton *et al.* [8] through X-ray diffraction studies. The Buchner *et al.* study found that with increasing absorbed hydrogen content there was an increase in the lattice parameter from 3.01 to 3.10 Å (a 9% volume increase). The Pelton *et al.* study found that an increase in hydrogen content from 20 to 1050 wppm produced an increase in the lattice parameter from 3.025 to 3.047 Å (a 2.2% volume increase). This study also found that the XRD peaks decreased in intensity with increased hydrogen content indicating hydrogen-induced lattice strain.

The effect of hydrogen on the austenite and martensite transition temperatures was investigated by B.L. Pelton *et al.* [2]. The study focused on NiTi samples with hydrogen concentrations from 400 to 1809 wppm. DSC analyses found that as the hydrogen content increased from to 1809 wppm from 3 wppm in the baseline material, the phase transitions shifted to lower temperatures and the

enthalpies of the reactions were decreased. Both the austenite and martensite transitions were completely suppressed by the 1809 wppm hydrogen content.

The study by B.L. Pelton *et al.* [2] also examined the fracture mode of hydrogen-charged NiTi samples. The baseline sample with 3 wppm hydrogen displayed a ductile cup-cone fracture surface and the sample with 1809 wppm displayed a brittle fracture band at the surface on the material. Samples containing hydrogen contents between 3 and 1809 wppm showed the brittle fracture band increasing in width, up to 130 mm in the 1809 wppm sample, with increasing hydrogen content.

Materials and Experimental Methods

Hydrogen-charged samples of Ni_{50.8}Ti_{49.2} strip were prepared to study the effect of increasing hydrogen content on the phase stability of NiTi. The strip samples were mechanically polished, annealed, and chemically polished prior to the hydrogen-charging procedure. The samples were placed in an electrochemical cell in a mixture of phosphoric and hydrofluoric acid for hydrogen-charging. The samples were charged at temperatures between 5°C and 35°C, voltages between 3 and 15 volts, and times between 5 and 600 seconds. These charging conditions produced hydrogen concentrations between 32 wppm and 662 wppm. Charged samples were sent to Luvak, Inc. (Boylston, MA) for bulk hydrogen analysis using the vacuum hot extraction test method.

X-ray diffraction analyses were performed on the baseline material (i.e., no H charging) and hydrogen charged samples. The analyses were done using a Siemens Kristalloflex D5000 X-ray diffractometer. The XRD scans were run using a copper K_α X-ray source, a nickel filter, and NIST Standard Reference Material 640c silicon powder as a standard. Each scan collected data from 18° to 150° 2θ at an increment of 0.01° and a scan speed of 25 sec/increment. The austenite peaks from each XRD scan were used to calculate the B2 cubic lattice parameter. The lattice constant was plotted versus cos²θ/sinθ for B2 peaks in each sample, and an extrapolation was used to determine the lattice parameter for each sample [9].

Differential scanning calorimetry analyses were performed on the baseline material and hydrogen-charged samples with hydrogen contents from 32 wppm to 240 wppm. The analyses were done using a Seiko Instruments EXSTAR 6000 DSC 6200. For each DSC scan, the sample was first heated to 125°C to drive off water vapor. Data was then collected as the sample was cooled from 125°C to -125°C and heated from -125°C to 125°C at a rate of 5 deg/min. The DSC scans were used to determine the martensite and austenite transition temperatures and the phase transition enthalpies.

Tensile tests were performed on the baseline material and samples charged with 51 wppm, 102 wppm, and 180 wppm hydrogen. Data from the tensile tests were used to determine the effect of hydrogen on the mechanical properties of the NiTi strip. The fracture surfaces of the tensile samples were examined using scanning electron microscopy (SEM) for changes in the fracture mode. In addition, a sample with 483 wppm hydrogen was snapped by bare hands, and the fracture surface was examined.

Results and Discussion

X-Ray Diffraction

X-ray diffraction analysis was done on electropolished baseline material with a hydrogen content of 9 wppm and hydrogen-charged samples with hydrogen contents ranging from 100 wppm to 650 wppm. The B2 peaks from the XRD scans were used to calculate the lattice parameter for each sample. Figure 1 shows the XRD scans for the baseline material, a sample charged with 240 wppm hydrogen, and a sample charged with 647 wppm hydrogen from approximately 38° to 47° 2θ . The scans show a shift in the $\{110\}_{B2}$ peak to lower 2θ angles with increasing hydrogen content. The peak shift corresponds to a lattice parameter increase from 3.011 to 3.018 Å, a 0.7% volume increase from the baseline material with 9 wppm hydrogen to the high H-content sample with 647 wppm hydrogen. The peak shift and corresponding volume increase are consistent with the results reported by Pelton *et al.* [8].

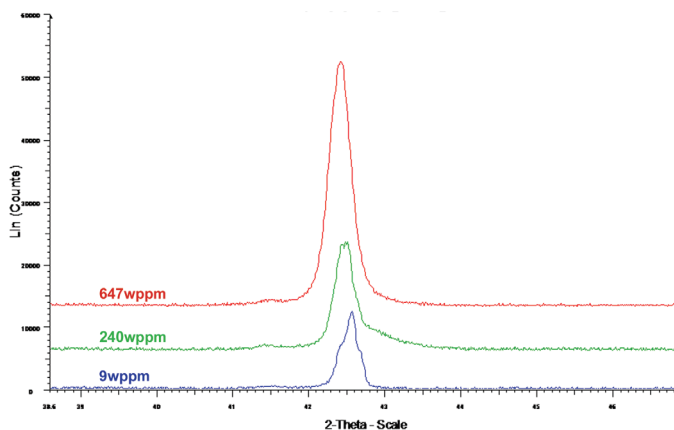


Figure 1. XRD scans of annealed and hydrogen-charged NiTi strip showing the $\{110\}_{B2}$ peak. The peak shifts to lower 2θ angles with increasing hydrogen content.

Differential Scanning Calorimetry

DSC analyses were done on NiTi samples with hydrogen contents from the baseline value of 9 wppm to 240 wppm. Figure 2 shows the DSC scans for the baseline material, a sample with 97 wppm hydrogen, and a sample with 190 wppm hydrogen. The scans show a suppression of the austenite peak during heating and a more significant suppression of the martensite peak during cooling. Not only do the DSC peaks decrease in magnitude, but the austenite to martensite transition temperature dramatically shifts to much lower temperatures.

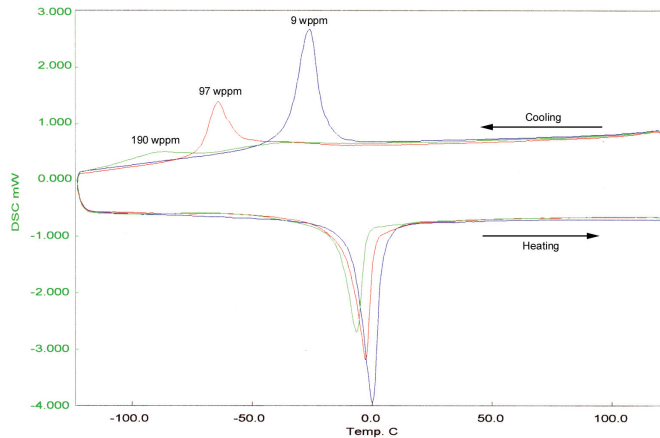


Figure 2. DSC scans of annealed and hydrogen-charged NiTi strip. Increasing hydrogen content suppresses both the austenite and martensite transitions.

Figure 3 shows the effect of increasing hydrogen content on the austenite transition temperatures. From the baseline material with a hydrogen content of 9 wppm hydrogen to a sample charged with 240 wppm hydrogen, the A_s temperature was lowered by approximately 8°C and the A_f was lowered by approximately 9°C. The enthalpy of the austenite transition was also decreased with hydrogen content. Figure 4 shows the decrease in enthalpy observed with increasing hydrogen. The enthalpy was decreased significantly between 200 and 240 wppm hydrogen. The total decrease in the austenite transition enthalpy was approximately 13 mJ/mg. No austenite transition was observed in samples with hydrogen contents above 240 wppm. Rather than the transformation becoming easier, the decrease in enthalpies is attributed to less of the transition occurring throughout the NiTi sample.

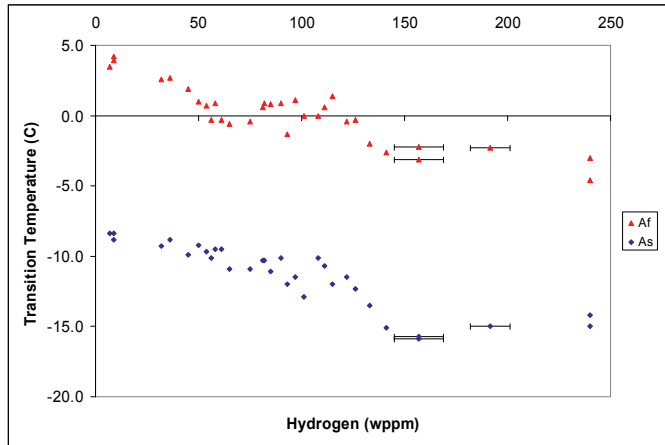


Figure 3. Plot showing the effect of increasing hydrogen content on the austenite transition temperatures.

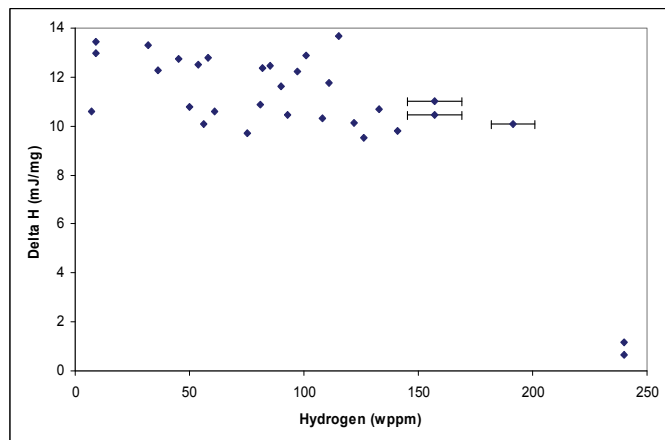


Figure 4. Plot showing the effect of increasing hydrogen content on the austenite transition enthalpy.

Increasing the hydrogen content had a more significant effect on the martensite (A→M) transition than the austenite transition (M→A). Figure 5 shows the effect hydrogen had on the martensite transition temperatures. From the baseline material with a hydrogen content of 9 wppm hydrogen and a sample charged with 200 wppm hydrogen, the M_s temperature was lowered by approximately 80°C and the M_f was lowered by approximately 110°C. The enthalpy of the martensite transition was also affected more significantly than that of the austenite transition. Figure 6 shows the change in enthalpy observed in the martensite transition with a total decrease of approximately 11 mJ/mg. Although the total enthalpy decrease during the martensite transition was less than that seen in the austenite transition with both peaks eventually disappearing, the martensite transition was lost at a lower hydrogen content than the austenite

transition. No martensite transition was observed in samples with hydrogen contents above 200 wppm. Again, the decrease in enthalpies is attributed to the suppression and eventual disappearance of the phase transition in NiTi.

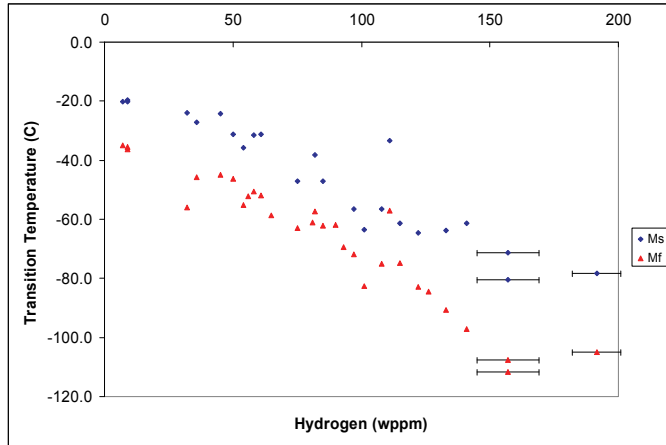


Figure 5. Plot showing the effect of increasing hydrogen content on the martensite transition temperatures.

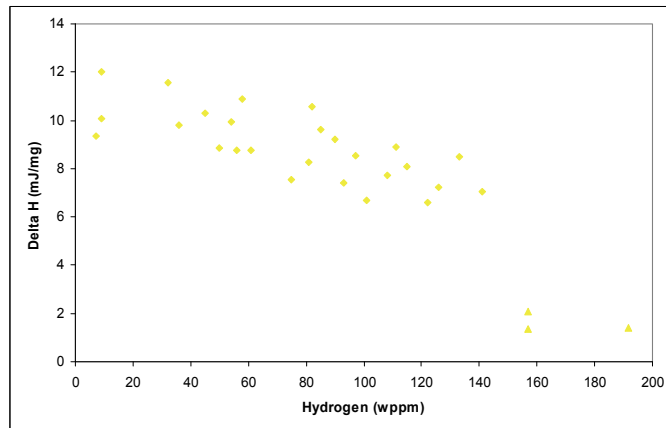


Figure 6. Plot showing the effect of increasing hydrogen content on the martensite transition enthalpy.

The decrease in the transition temperatures and enthalpies, particularly those of the martensite phase, indicate that hydrogen has a significant effect on the phase stability of NiTi. It appears that the austenite phase is stabilized as the hydrogen content increases.

Tensile Tests and Fracture Analysis

Figure 7 shows tensile test graphs for the baseline material and hydrogen-charged samples with hydrogen contents of 51 wppm, 102 wppm, and 180 wppm. The graph shows an increase in the martensite stress plateau due to increased hydrogen content from approximately 330 MPa in the baseline material to approximately 390 MPa in the hydrogen-charged samples. The increase in the martensite stress plateau suggests that with hydrogen contents above the 9 wppm in the baseline material, more energy is required for the austenite to martensite transition, which is consistent with the stabilization of the austenite phase.

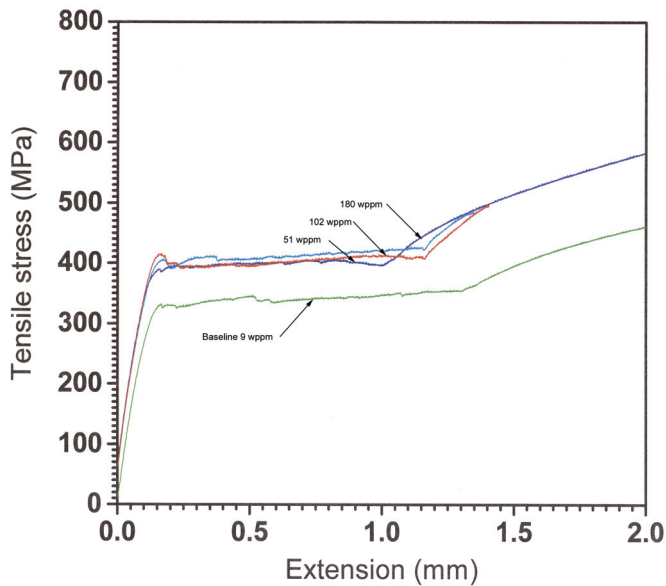


Figure 7. Tensile test graphs showing an increase in the martensite stress plateau with increased hydrogen content.

Scanning electron microscopy was used to examine the surfaces of the fractured tensile samples and of a sample charged with 483 wppm hydrogen that snapped in half. Figures 8a-e show the fracture surfaces of the baseline and hydrogen-charged samples. The fracture surfaces reveal that as hydrogen content is increased, the fracture mode transitions from a ductile cup-cone mode in the baseline sample to a brittle transgranular mode in the 483 wppm hydrogen sample. While a significant portion of the fracture surface appears brittle by the 102 wppm hydrogen content sample, none of the surfaces exhibited increasing brittle fracture bands at the surface as seen by Pelton *et al.* [2].

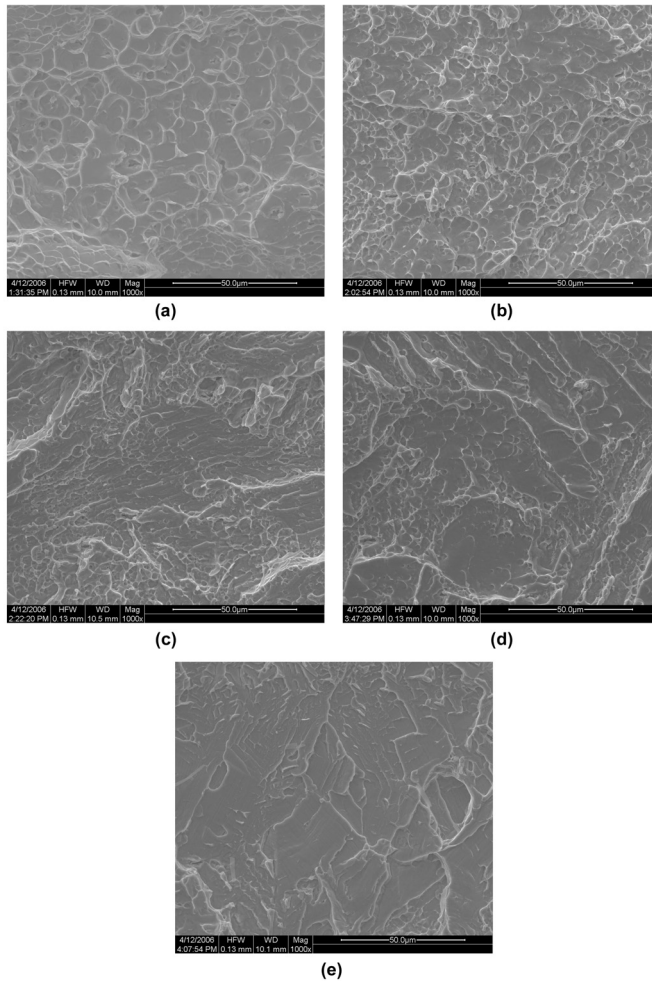


Figure 8. SEM images of fracture surfaces of NiTi samples with different hydrogen contents: (a) 9 wppm (b) 51 wppm (c) 102 wppm (d) 180 wppm and (e) 483 wppm that show an increase in brittle fracture mode. All images are at the same magnification.

DSC and tensile test analyses suggest that increasing hydrogen content stabilizes the austenite phase through suppression of the austenite to martensite phase transition. The lowered martensite transition temperatures and increased martensite stress plateau indicate that the suppression of the transition ($A \rightarrow M$) occurs at hydrogen contents as low as 50 wppm, the upper limit for hydrogen content set in the NiTi ASTM materials specification [10]. Since these low hydrogen contents have been shown to have a suppressive effect on the phase transition central to nearly all applications of Nitinol, it is important to recognize and be conscious of the hydrogen content present in NiTi shape memory alloys and how it may be affecting the fundamental phase transition property.

Summary and Conclusions

This study showed that hydrogen has a significant effect on the phase stability of NiTi strip (that has been annealed and hydrogen charged) through X-ray diffraction, differential scanning calorimetry, and tensile testing. The following are preliminary conclusions of the study:

1. XRD analyses showed that as hydrogen content increased, the B2 peaks shifted to lower 2θ angles, corresponding to an increase in the lattice parameter from 3.011 to 3.018 Å. The lattice parameter increase represents a 0.7% cubic volume increase.
2. DSC analyses showed a decrease in transition temperatures and enthalpies for both the austenite and martensite transitions. With an increase of hydrogen content from 9 to 240 wppm, the A_s temperature was suppressed 8°C and the A_f was suppressed 9°C. The transition temperature and enthalpy decrease was more significant for the martensite phase with the M_s suppressed 80°C and the M_f suppressed 110°C. The decline in enthalpies was attributed to the suppression and eventual loss of the austenite to martensite transition with increased hydrogen content.
3. Tensile tests showed an increase of approximately 60 MPa in the induced martensite stress plateau with hydrogen contents (at least 50 wppm) greater than the baseline value of 9 wppm.
4. SEM images of the fracture surfaces of baseline material and hydrogen-charged samples showed that increasing hydrogen content results in an increasingly brittle fracture mode.

Observations from the DSC analyses and tensile tests indicate that hydrogen stabilizes the austenite phase. With increasing amounts of hydrogen the austenite to martensite transition is suppressed, and virtually disappears with a hydrogen content of approximately 240 wppm.

References

1. A.W. Thompson and N.R. Moody, eds., *Hydrogen Effects in Materials* (Warrendale, Pa: TMS, 1996), pp 699-840.
2. B.L. Pelton, T. Slater, and A.R. Pelton, in *SMST-97: Proceedings of the Second International Conference on Shape Memory and Superelastic Technologies*, eds. A.R. Pelton *et al.* (Pacific Grove, CA: International Organization on SMST), pp 395-400.
3. T. Asaoka, H. Saito, and Y. Ishida, in *Proc. ICOMAT* (1993), p. 1003.
4. K. Yokoyama *et al.*, *Biomaterials* **22** (2001), p. 2257.
5. T. Asaoka, in *SMST-94: Proceedings of the First International Conference on Shape Memory and Superelastic Technologies*, eds. A.R. Pelton *et al.* (Pacific Grove, CA: International Organization on SMST), p. 79.
6. T. Asaoka, *J. de Physique IV*, C8, 1995, p. 723.
7. H. Buchner *et al.*, *Z. Metallkunde* 63 (1972), p. 497.
8. A.R. Pelton *et al.*, in *SMST-2003: Proceedings of the International Conference on Shape Memory and Superelastic Technologies*, eds. A.R. Pelton *et al.* (Pacific Grove, CA: International Organization on SMST), pp 33-42.
9. C. Suryanarayana and M. Grant Norton, *X-Ray Diffraction A Practical Approach* (New York, NY: Plenum Press, 1998), pp 153-166.
10. ASTM F 2063 – 00: *Standard Specification for Wrought Nickel-Titanium Shape Memory Alloys for Medical Devices and Surgical Implants*, 2000.